



Published in final edited form as:

Acta Biomater. 2017 July 15; 57: 324–333. doi:10.1016/j.actbio.2017.05.015.

TOWARDS REBUILDING VAGINAL SUPPORT UTILIZING AN EXTRACELLULAR MATRIX BIOSCAFFOLD

Rui Liang, MD^{1,3}, Katrina Knight, BS², Deanna Easley, BS², Stacy Palcsey, BS¹, Steven Abramowitch, PhD^{1,2}, and Pamela A. Moalli, MD PhD^{1,2,3}

¹Magee Women Research Institute, University of Pittsburgh, Pittsburgh, PA, USA

²Department of Bioengineering, University of Pittsburgh, Pittsburgh, PA, USA

³Department of Obstetrics, Gynecology, and Reproductive Sciences, School of Medicine, University of Pittsburgh, Pittsburgh, PA, USA

Abstract

As an alternative to polypropylene mesh, we explored an extracellular matrix (ECM) bioscaffold derived from urinary bladder matrix (MatriStem™) in the repair of vaginal prolapse. We aimed to restore disrupted vaginal support simulating application via transvaginal and transabdominal approaches in a macaque model focusing on the impact on vaginal structure, function, and the host immune response. In 16 macaques, after laparotomy, the uterosacral ligaments and paravaginal attachments to pelvic side wall were completely transected (IACUC# 13081928). 6ply MatriStem was cut into posterior and anterior templates with a portion covering the vagina and arms simulating uterosacral ligaments and paravaginal attachments, respectively. After surgically exposing the correct anatomical sites, in 8 animals, a vaginal incision was made on the anterior and posterior vagina and the respective scaffolds were passed into the vagina via these incisions (transvaginal insertion) prior to placement. The remaining 8 animals underwent the same surgery without vaginal incisions (transabdominal insertion). Three months post implantation, firm tissue bands extending from vagina to pelvic side wall appeared in both MatriStem groups. Experimental endpoints examining impact of MatriStem on the vagina demonstrated that vaginal biochemical and biomechanical parameters, smooth muscle thickness and contractility, and immune responses were similar in the MatriStem no incision group and sham-operated controls. In the MatriStem incision group, a 41% decrease in vaginal stiffness ($P=0.042$), a 22% decrease in collagen content ($P=0.008$) and a 25% increase in collagen subtypes III/I was observed vs. Sham. Active MMP2 was increased in both MatriStem groups vs. Sham (both $P=0.002$). This study presents a novel application of ECM bioscaffolds as a first step towards the rebuilding of vaginal support.

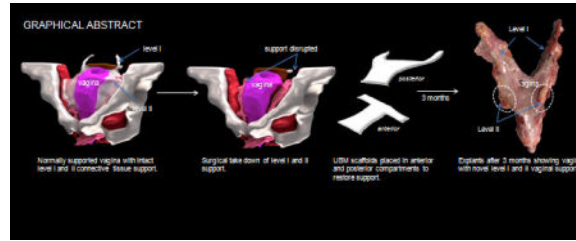
Corresponding author: Pamela A. Moalli MD PhD, Magee Women Research Institute, Department of Obstetrics and Gynecology, 204 Craft Ave., Pittsburgh, PA 15219, Phone: 1-412-641-6012, Fax: 1-412-641-5290, moalpa@mail.magee.edu.

Publisher's Disclaimer: This is a PDF file of an unedited manuscript that has been accepted for publication. As a service to our customers we are providing this early version of the manuscript. The manuscript will undergo copyediting, typesetting, and review of the resulting proof before it is published in its final citable form. Please note that during the production process errors may be discovered which could affect the content, and all legal disclaimers that apply to the journal pertain.

Disclosures

RL, SP, SA and PAM received partial salary support from their institute cooperative research agreement with ACell®, Inc. (Columbia, MD, USA). KK, and DE have no conflict of interest.

Graphical abstract



Keywords

Prolapse; Extracellular matrix; Vaginal incision; Pelvic support; Regeneration

1. Introduction

Vaginal prolapse also known as pelvic organ prolapse (POP), is a common condition in which loss of soft tissue support to the vagina causes the organs supported by it (bladder, uterus, small bowel and rectum) to herniate or fall into the vaginal lumen causing significant physical discomfort and psychological distress to affected women. Support to the upper and mid-vagina is provided by the uterosacral ligaments and paravaginal attachments to the pelvic side-wall, respectively. The vagina and supportive tissues of women with prolapse have been shown to be structurally and functionally compromised with altered collagen and elastin content [1–3], increased tissue degrading proteases [2], disorganization and atrophy of smooth muscle [4, 5] and inferior mechanical properties [6]. Up to 12.6% of women will undergo a surgery to repair prolapse by age 80 [7]. Of those who undergo a native tissue repair, 40% will fail by 2 years [8, 9][10].

In response to the high failure rates associated with native tissue repairs, surgeons have turned to lightweight polypropylene mesh. In spite of fairly good anatomical outcomes, polypropylene prolapse meshes have been associated with numerous complications, most commonly mesh exposure through the vaginal epithelium, pain, and erosion into adjacent structures [11], prompting 2 FDA warnings and an upclassification of meshes from Class II to Class III devices [12]. In nonhuman primates, Gynemesh PS - the prototype and most widely implanted polypropylene prolapse mesh, has been shown to have a negative impact on the vagina inducing a robust long-term foreign body response associated with degeneration and atrophy, and a loss of functional integrity [13, 14]. Thus, regenerative techniques that direct the host to rebuild and restore damaged vaginal soft tissue support structures represent a viable alternative approach.

Bioscaffolds derived from extracellular matrix (ECM) have been widely adopted in tissue engineering applications and are considered a novel tool in tissue regeneration. They have been shown to promote tissue regeneration in different tissues, e.g. skeletal muscle, tendon, fibrocartilage, and digits, in numerous preclinical animal studies and human clinical applications by facilitating a site-specific constructive tissue remodeling response [15]. When placed in the appropriate *in vivo* mechanical loading environment, the remodeling of

ECM bioscaffolds is directed to promote the formation of a site specific tissue with robust mechanical properties [16–18]; a scenario seemingly perfectly aligned with the goals of patients and surgeons – that is, to repair the damaged/impaired vagina and its supportive tissues in patients with prolapse.

Restoration of apical (level I) and lateral (level II) support to the vagina has been shown to be key in achieving successful anatomical outcomes in the long term [19–21]. Therefore, the overall goal of this study was to determine the feasibility of utilizing a regenerative ECM bioscaffold in prolapse applications to restore uterosacral ligaments (level I) and paravaginal attachments into the pelvic side wall (level II) without negatively impacting vaginal structure and function (Figure 1). Secondly, since the approach by which surgical material is delivered to the host has been shown to impact outcomes with transvaginal applications associated with higher rates of complications than transabdominal applications [22–24], we modeled and compared these two approaches for bioscaffold placement. We chose MatriStem (porcine urinary bladder matrix, ACELL), a noncrosslinked degradable acellular ECM bioscaffold because of its ability to promote the growth of tissue containing both smooth muscle and matrix [25–28], two critical components of the vagina and the soft tissues that support it. We used a 6-ply scaffold since we arguably needed a graft that had similar initial mechanical integrity to commonly used prolapse meshes [13, 29] that would persist as it was slowly replaced with host newly formed tissues. Since complications following prolapse procedures typically involve the vagina (exposure and pain), we sought to focus the current study on the impact of MatriStem on vaginal morphology, biochemical composition, and function (passive and active mechanics). Moreover, we were concerned about stress shielding effects given that the 6-ply MatriStem bioscaffold had an initial structural stiffness similar to synthetic prolapse meshes and therefore, could potentially exert a negative impact on the vagina due to stress shielding [13]. The rhesus macaque model was used due to its marked similarities to humans. Previous studies have demonstrated a prolonged foreign body response with synthetic meshes and crosslinked biologic materials; thus, the host immune response was also assessed [22–24].

2. Materials and Methods

2.1 Animals

Rhesus macaques (*macacca mulatta*) used in this study were maintained and treated according to experimental protocols approved by the Institutional Animal Care Use Committee of the University of Pittsburgh (IACUC #13081928) and in adherence to the National Institutes of Health Guidelines for the use of primates as “an acutely scarce resource” such that a minimum number were used for meaningful results. Routine laboratory tests and regular examinations by veterinarians during a quarantine period were used to certify that these experimental animals were pathogen-free and in good physical condition. Animals were maintained in standard cages with ad libitum water and a scheduled monkey nutritious diet. A 12-hour light/dark cycle (7 am to 7 pm) was used, and menstrual cycle patterns were recorded daily. Age, weight, and parity were collected prior to and after surgery.

2.2 Surgical procedures

For comparison of our experimental endpoints, we used previously published data for Sham (n=12). These animals had been operated in the same way as our MatriStem implanted animals with surgical exposures affording the implantation of a vaginal graft but did not undergo disruption of level I and II support or the application of the bioscaffold [13, 14]. Our decision to use control animals without disrupted support is based on our previous finding that the prolapsed unsupported vagina has inferior mechanical properties, altered collagen ratios and increased active MMP-9 [30, 31] relative to the vagina with intact support. In this way, by comparing to normally supported animals, we would be comparing our MatriStem implanted vagina to the “gold standard”. After laparotomy, [31]16 rhesus macaques underwent a hysterectomy followed by complete transection of the uterosacral ligaments (level I) and paravaginal attachments to pelvic sidewall (level II) (Figure 2). The bladder and rectum were sharply dissected off of the vagina to expose the full thickness vaginal wall. A 6ply MatriStem scaffold was cut into posterior and anterior templates with a vaginal portion and arms to simulate uterosacral ligaments and paravaginal attachments, respectively (Figure 3). To model transvaginal insertion (N=8), a 3cm vaginal incision was made on both the anterior and posterior vaginal walls and the respective scaffolds placed into the vaginal lumen via these incisions where they were held there for ~ 5 minutes before pulling back into the pelvic cavity. Vaginal incisions were then repaired with 2-0 Vicryl. The remaining animals (N=8) underwent the same surgery without vaginal incisions to model a transabdominal insertion. The scaffolds were sutured to the vagina, the arms placed in the anatomically correct positions for level I and II support and then retroperitonealized. For rebuilding level I support (the uterosacral ligaments), the scaffold arms were placed into the fibrous portion of the pubocaudalis muscle at the sacrum adjacent to S1-S2. For level II support (paravaginal attachments), the arms were placed at the level of the mid vagina into the site analogous to the arcus tendineous fascia pelvis; that is, at the junction between the pubocaudalis and the obturator internus muscles. The arms were sewn in place using 3-0 delayed absorbable suture (3-0 polydioxanone suture). At 3 months post-surgery, the gross morphology was observed and grafted vagina was harvested for the following tests.

2.3 Ball-burst test for biomechanical properties

The passive mechanical properties of the grafted vagina were determined by ball burst testing as described previously [13]. Sixteen samples from transvaginal groups with incision (n=8) and without incision (n=8) were tested. Tissues were handled with care, wrapped in saline soaked gauze and then stored at -20° C until day of testing [32, 33]. As the ball burst protocol tests a standardized size of tissue, the data was not normalized and there were no differences in thickness between groups as measured using a laser reflectance system [13]. Structural properties including stiffness (N/mm), ultimate load (N), ultimate elongation (mm), and energy absorbed (N/mm) were determined. For these samples, it was assumed that Matristem completely degraded during the implantation period (3 months) [34], or if partially degraded, the remnants possessed no independent mechanical integrity at the time of tissue procurement.

2.4 Functional test for smooth muscle contractility

The contractile response to a single dose of KCl (120mM) was tested within 30 minutes of tissue harvest as described previously [35]. In order to normalize for differences in tissue quantity, the data was expressed as force per muscle volume of each strip (mN/mm^3). Strips were then washed and exposed to electrical field stimulation (EFS) at only one voltage (20 V) for a duration of 5 seconds, and the frequency was increased from 1–64 Hz. For EFS, the contractile force was normalized by the 120 mM KCl response and expressed as a percentage. Only the maximum force generated for each strip was reported for EFS.

Immunofluorescent labeling of alpha smooth muscle actin (α -SMA) and in situ TUNEL labeling of apoptotic cells—The grafted vagina was embedded in O.C.T. compound (Sakura Finetek USA, Inc, Torrance, CA) and cryosectioned ($7\mu\text{m}$). The tissue was oriented with the sectioned aspect cut perpendicular to the vagina. H&E and Masson's trichrome staining were first performed to examine the integrity of the tissue and the inflammatory responses in the mesh area. Tissue blocks that did not achieve the correct orientation requisite for quantitative analysis, i.e. not containing full thickness vagina, obliquely sectioned with subepithelium thicker than $1039\mu\text{m}$ (mean of Sham values that were ensured perpendicular sectioning plus 2 standard deviation) were excluded. No samples in the MatriStem groups were excluded. Procedures and quantification of thickness of the subepithelium and smooth muscle layer as well as the percentage of apoptotic cells in different tissue layers was performed as described previously [14].

2.5 Immunofluorescent labeling of macrophages

To determine whether MatriStem elicited a long-term immune response similar to other biomaterials used in prolapse surgeries [36, 37], our previous method for immunolabeling macrophages and differentiating M1 (proinflammatory) and M2 (remodeling) macrophages was followed [36]. Tissue sections were triple-labeled with antibodies specific for a pan-macrophage marker (CD68), an M1 marker (CD86), and an M2 marker (CD206). Slides were imaged using a 20X objective. CD68+CD86+ cells were considered to have an M1 phenotype and CD68+CD206+ cells were considered to have an M2 phenotype. Cell counts were averaged for each sample and expressed as a percentage of total cells within a 20X field.

2.6 Hydroxyproline assay

The grafted vagina were harvested and dried. Total collagen content was measured using the hydroxyproline assay as previously described [38]. The collagen content was estimated by assuming that 14% of collagen (weight) is hydroxyproline and expressed by percentage of tissue dry weight. Each animal was sampled three times and the experiment was repeated at least in triplicate.

2.7 UPLC Desmosine and Isodesmosine measurement for mature elastin

Mature elastin content was measured by ultrahigh performance liquid chromatography (UPLC) as previously described [39, 40]. Briefly, hydrolyzed tissue was applied to Oasis MCX cation exchange SPE columns (Waters, Milford Massachusetts), and eluted with

ammonium hydroxide/water/methanol (10/40/50). Stock solutions of desmosine, isodesmosine and S-[beta-(4-pyridyl)ethyl]L-cysteine (internal standard, S-LC) (Santa Cruz, Dallas, Texas) were diluted to series concentration to create standard curves. S-LC (2 μ mol) was added to each sample and standard as an internal control. Three μ l of the prepared samples and standards were injected onto a prepared Waters Acquity UPLC BEH C18 column and monitored by measuring absorbance at 270nm wavelength. Elution time of isodesmosine was at 1.4 min, desmosine at 1.9 min and S-LC at 2.4 min. The amount of mature elastin in each sample was represented by the sum of desmosine (μ mol/L) and isodesmosine (μ mol/L) and estimated by assuming that 1.3% of mature elastin (weight) is desmosine and isodesmosine [41]. The results were expressed as percentage of tissue dry weight. It should be noted that the amount of desmosine and isodesmosine in mature elastin varies in different tissues and species [42] and that the adopted conversion value above was derived from human aorta and lung.

2.8 1, 9-Dimethylmethylene Blue assay

Total content of sulfated glycosaminoglycans (GAG) was measured using the 1,9-Dimethylmethylene Blue assay as previously described [43]. The content of GAG was determined with respect to the tissue dry weight.

2.9 Interrupted SDS-PAGE for collagen subtypes

Previous methods were followed to determine the ratios of collagen subtype III/I in the mesh tissue complex [44]. The relative collagen subtype III/I ratio was determined and calculated as $\alpha 1(\text{III}) \times 2 / \alpha 1(\text{I}) \times 3$.

2.10 Gelatin zymography for MMPs -2, and -9

The expression of matrix degrading enzymes, MMPs-2 and -9, was evaluated using substrate zymography with 30 μ g of proteins per sample. The experiment was carried out in duplicate with a pre-cast 10% gelatin gel system (Invitrogen, Carlsbad, CA) as described previously [31].

2.11 Statistical analysis

Sample size was determined using previous published mechanical data (ultimate load and stiffness) for Sham and a synthetic mesh implantation - Gynemesh PS, in which at least 8 animals were needed in each group to find significance with α error of 0.05 and power of 0.80. Data was tested for distribution before statistical analysis. For normally distributed data, a oneway analysis of variance (ANOVA) was used followed by the appropriate post-hoc tests including Dunnett's for comparison to Sham and pair-wise test using Bonferroni multiple comparisons procedure between all groups. For nonparametric data, Kruskal-Wallis and Mann-Whitney tests were used.

3. Results

Animals were middle-aged with similar weight and parity (Table 1). Animals in the MatriStem groups were younger than Sham (both $p=0.002$); however, multivariate

regression modeling showed that age had no significant predictive value for any of the parameters in the study. Therefore, the results were not adjusted for the impact of age.

3.1 Gross morphology

Pelvic exam demonstrated that the vagina was well supported in all groups in which the MatriStem grafts had been placed. At necropsy, newly formed tissue bands were observed at the site of implantation of the bioscaffold arms bilaterally at the vaginal apex extending along the pelvic sidewall toward the sacrum and at the mid- vagina inserting into the pelvic sidewall (Figure 4). These bands appeared broad and contained both fibrous and fatty tissue and were well vascularized consistent with a connective tissue. The vagina appeared grossly normal. There was no evidence of residual graft. As the main focus of the study was to define the impact of MatriStem on the vagina, the remaining experimental endpoints are focused on the portion of the vagina where MatriStem had been placed.

3.2 Biomechanical properties of the vagina

With ball-burst testing, rupture of the grafted vagina occurred at the point of contact with the ball head in all samples. When compared to Sham, the overall structural properties of grafted vagina implanted with MatriStem with and without an incision were not significantly different (Table 2). Yet, it is notable that the stiffness of the grafted vagina in the MatriStem transvaginal insertion group was 41% lower than that in Sham ($P=0.042$), indicating a negative impact with a vaginal incision.

3.3 Vaginal inflammatory responses and cell apoptosis

With H&E and trichrome staining, no obvious difference was observed between MatriStem groups and Sham independent of the presence or absence of an incision (Figure 5). Infiltration of inflammatory cells was not apparent. Of the few macrophages present, the CD68+CD206+ M2 remodeling subtype was predominant relative to CD68+CD86+ M1 subtypes. No increase in the number of apoptotic cells was observed in any of the three layers of vagina (subepithelium, muscularis and adventitia) for both MatriStem groups when compared to Sham (Table 3).

3.4 Vaginal Smooth muscle morphology and contractility

Overall, the thickness of subepithelium in the three groups was similar (overall $P=0.064$, Table 3). The contour of smooth muscle layer was clearly demarcated after labeling with α -SMA in all samples (Figure 5). Semi-quantitative histomorphometric measurement of the thickness of smooth muscle layer in the vagina showed MatriStem implanted in the presence and absence of an incision did not impact the thickness of muscle layer as compared to Sham (overall $P=0.747$, Table 3). Functionally, in contrast to what has been observed following the implantation of polypropylene mesh, the contractile force generated in response to KCL was similar between MatriStem groups and Sham (overall $P=0.154$, Table 3). In addition, no significant differences in nerve mediated contractions as shown by electrical field stimulation was observed among the 3 groups (overall $P=0.797$, Table 3).

3.5 Biochemical analysis of vaginal ECM components

Total collagen content was decreased in the MatriStem implanted groups (overall $P=0.016$, Table 4) relative to Sham. Specifically, in the presence of MatriStem with a vaginal incision, a 22% decrease in collagen was observed comparing to Sham ($P=0.008$) paralleling the trend toward a decrease in stiffness observed in the mechanical testing. No significant difference was observed between MatriStem without an incision and Sham indicating that the incision was having an independent effect ($P=0.304$). In addition, the ratio of collagen subtype III to I in the vagina was increased by 25% following MatriStem insertion in the presence of an incision as compared with Sham ($P=0.038$, Table 4 and Figure 6). Such an increase was not observed in the MatriStem no incision group ($P=0.088$) indicating that again the presence of an incision was negatively impacting outcomes. Mature elastin content and sulfated GAG content were not significantly different between the groups (Table 4).

3.6 Zymography of MMP-2 and -9

Both proenzymatic and active forms of MMP-2 and -9 were visualized by substrate zymography (Figure 6). Semi-quantitative analysis of MMP-2 and -9 indicated that active MMP-2 and the ratio of active and proenzyme form of MMP-2 (A/P MMP-2) were both significantly increased with MatriStem implantation regardless of the presence or absence of an incision as compared to Sham (overall $P=0.005$, 0.003 , respectively). Specifically, the active form of MMP-2 increased by 2 to 3 fold ($P=0.011$ with and 0.003 without an incision) and the A/P MMP-2 increased 4 to 5 fold ($P=0.002$ with and 0.002 without incision, respectively) in the MatriStem groups relative to Sham. Proenzymatic and active form of MMP-9 were not significantly different between groups.

4. Discussion

This study explored the use of MatriStem, an extracellular matrix (ECM) bioscaffold derived from urinary bladder matrix, as a first step towards regenerating disrupted level I and II vaginal support in nonhuman primates with an in depth analysis of the impact of this multi-layered scaffold on the vagina. We observed that newly formed tissue bands were present in the position where the bioscaffold arms had been placed at the vaginal apex (level I) and paravaginal attachments to the pelvic sidewall (level II) at the mid vagina. We show that, in spite of having an initial structural stiffness similar to that of commonly used prolapse meshes [13, 29], MatriStem did not negatively impact the overall structure and function of the grafted vagina when placed in the absence of a vaginal incision (transabdominal model). This is in sharp contrast to our analyses of the vagina grafted with the polypropylene mesh (Gynemesh PS), which showed significant degenerative changes including a prolonged inflammatory response, increased cell apoptosis, decreased smooth muscle volume and contractility, and decreased fibrillar matrix associated with increased degradation and inferior mechanical properties [13, 14]. Implantation of MatriStem in the presence of a vaginal incision to model transvaginal insertion resulted in a reduced collagen content, decreased vaginal mechanical properties, increased collagen subtype III/I ratio and increased MMP-2 activity, suggesting a picture of ongoing healing and active remodeling. Longer time points following MatriStem insertion are needed to determine if the vagina eventually recovers to control levels after an incision is made. Clinically, the presence of a vaginal

incision increases the incidence of complications following the placement of polypropylene mesh [22–24].

The arms of the MatriStem bioscaffold were created to simulate the anatomical positions of level I and II vaginal support such that under physiological condition, the arms would be loaded similar to uterosacral ligaments (level I) and paravaginal attachments to pelvic side wall (level II). With the main portion attached to the vagina and the arms attached to anatomical insertion sites, our application provides a reasonable biological and mechanical environment for MatriStem to facilitate the regeneration of pelvic supportive tissues. While this study focused on the impact of MatriStem on the vagina, the observation of newly formed connective tissue bands in the position of normal vaginal support suggests that this is a promising approach that warrants further study in future prolapse repair applications.

The effects of ECM based bioscaffolds on facilitating constructive remodeling in damaged tissue have been well-documented [15]. With newer processing techniques, the ultrastructure and 3-D architecture of ECM bioscaffolds are largely preserved, providing a feasible microenvironment for cell migration, integration, differentiation and proliferation. ECM bioscaffolds are designed to degrade and to be gradually replaced by normal host tissue [45, 46][47–50][51]. MatriStem was chosen in this study because of its ability to facilitate the formation of smooth muscle in addition to fibrillar matrix in healing the disrupted esophagus and chronic wounds [25–28]. Importantly, the results of this study are based on animals with a surgically induced prolapse. Thus, if women with prolapse have genetically deficient or inherently altered ability to promote the growth of healthy tissue, it is unlikely that MatriStem would be effective. Small clinical trials using this product in women with prolapse will address this issue.

Our finding that MatriStem applied via a vaginal incision was associated with a decreased vaginal collagen content, increased ratio of collagen III/I, and a decreased stiffness relative to Sham, suggests that a vaginal incision may delay or permanently compromise healing and tissue remodeling in the grafted vagina. A transient decrease in tissue mechanical strength has been observed at early stage following a 8-ply SIS insertion to repair the abdominal wall in a dog model due to tissue remodeling [52]. It is not clear whether this process occurred in our animals but could present a period of vulnerability if used in prolapse repairs.

One of the major limitations of the study is that we were unable to justify the inclusion of a control group with disrupted support in this study. Thus, the question remains as to whether disrupted supportive tissues spontaneously reform in animals in the absence of MatriStem. Since completing the study, we have studied 2 animals in this “disrupted support” control group. At necropsy, 3 months after taking down level I and II support, although the vagina appeared supported in the supine position, we observed descent of the anterior and posterior walls with the application of suprapubic pressure. Filmy adhesions were observed in these control animals at the sites where suture had been placed with removal of the uterus. The sites where the uterosacral ligaments and paravaginal attachments had been disrupted, however, were replaced with a dense fat (see supplementary figure). While these observations are not quite visually different from a MatriStem mediated response, future studies with a larger control group will help to definitively answer this critical question.

Additional limitations include the number of animals used to answer our research question. We are keenly aware human primates are “an acutely scarce resource” and have powered our studies to use the smallest number of animals possible. This may account for the lack of statistical significance in some of the experimental endpoints, such as tissue stiffness. In addition, although prolapse is observed in the rhesus macaque [53], none of the animals in this study had prolapse more advanced than Stage II. To start with a similar amount of prolapse in our treatment groups, we surgically disrupted level I and II support. However, such an “acute” loss of support may not fully recapitulate all the anatomical defects leading to POP, particularly those in the levator ani muscles. Since the levator ani muscles clearly contribute to the support of the distal vagina and the caliber of the vaginal hiatus, it is not clear if MatriStem would have been as effective in restoring support to the vagina if the levator ani muscles had been injured as well. Finally, our study is cross-sectional and it is unclear whether the changes we observed at 3 months will persist over time. However, the study demonstrates that repair of disrupted supportive tissues of the vagina may be feasible and should serve as a launching pad for future studies.

5. Conclusion

Implantation of MatriStem did not negatively impact the overall functional, morphological and biochemical properties of the vagina when implanted in the absence of a vaginal incision. The presence of incisions compromised vaginal structural integrity with decreased collagen content at 3 month post-surgery possibly due to ongoing tissue healing and remodeling.

Supplementary Material

Refer to Web version on PubMed Central for supplementary material.

Acknowledgments

We thank Dr. Robert Powers (Magee-Womens Research Institute, Department of Obstetrics, Gynecology & Reproductive Biology, University of Pittsburgh) for his assistance in the mature elastin assay.

Funding: This work was supported by the NIH funding support R01 HD061811-01 and institute cooperative research agreement with ACell[®], Inc. (Columbia, MD, USA). The funding source had no involvement in the study design, collection of data, analysis of data, interpretation of data, writing of the report, or the decision to submit for publication.

References

1. Bildircin D, Kokcu A, Celik H, Sagir D, Kefeli M. Comparison of connective tissue components in the uterine ligaments between women with and without pelvic organ prolapse. *Minerva Ginecol.* 2014; 66:201–8. [PubMed: 24848078]
2. Chen B, Yeh J. Alterations in connective tissue metabolism in stress incontinence and prolapse. *J Urol.* 2011; 186:1768–72. [PubMed: 21944102]
3. Meijerink AM, van Rijssel RH, van der Linden PJ. Tissue composition of the vaginal wall in women with pelvic organ prolapse. *Gynecol Obstet Invest.* 2013; 75:21–7. [PubMed: 23108059]
4. Boreham MK, Miller RT, Schaffer JI, Word RA. Smooth muscle myosin heavy chain and caldesmon expression in the anterior vaginal wall of women with and without pelvic organ prolapse. *Am J Obstet Gynecol.* 2001; 185:944–52. [PubMed: 11641683]

5. Boreham MK, Wai CY, Miller RT, Schaffer JI, Word RA. Morphometric analysis of smooth muscle in the anterior vaginal wall of women with pelvic organ prolapse. *Am J Obstet Gynecol.* 2002; 187:56–63. [PubMed: 12114889]
6. Martins P, Lopes Silva-Filho A, Rodrigues Maciel da Fonseca AM, Santos A, Santos L, Mascarenhas T, Natal Jorge RM, Ferreira AJ. Biomechanical properties of vaginal tissue in women with pelvic organ prolapse. *Gynecol Obstet Invest.* 2013; 75:85–92. [PubMed: 23295833]
7. Wu JM, Matthews CA, Conover MM, Pate V, Jonsson Funk M. Lifetime risk of stress urinary incontinence or pelvic organ prolapse surgery. *Obstet Gynecol.* 2014; 123:1201–6. [PubMed: 24807341]
8. Barber MD, Brubaker L, Burgio KL, Richter HE, Nygaard I, Weidner AC, Menefee SA, Lukacz ES, Norton P, Schaffer J, Nguyen JN, Borello-France D, Goode PS, Jakus-Waldman S, Spino C, Warren LK, Gantz MG, Meikle SF. Comparison of 2 transvaginal surgical approaches and perioperative behavioral therapy for apical vaginal prolapse: the OPTIMAL randomized trial. *JAMA.* 2014; 311:1023–34. [PubMed: 24618964]
9. Siff LN, Barber MD. Native Tissue Prolapse Repairs: Comparative Effectiveness Trials. *Obstet Gynecol Clin North Am.* 2016; 43:69–81. [PubMed: 26880509]
10. Olsen AL, Smith VJ, Bergstrom JO, Colling JC, Clark AL. Epidemiology of surgically managed pelvic organ prolapse and urinary incontinence. *Obstet Gynecol.* 1997; 89:501–6. [PubMed: 9083302]
11. Maher, C., Feiner, B., Baessler, K., Schmid, C. Surgical management of pelvic organ prolapse in women; *Cochrane Database Syst Rev.* 2013. p. CD004014 <http://onlinelibrary.wiley.com/doi/10.1002/14651858.CD004014.pub5/pdf>
12. FDA. , editor. FSC. UPDATE on serious complications associated with transvaginal placement of surgical mesh for pelvic organ prolapse. Jul. 2011 <https://www.fda.gov/MedicalDevices/Safety/alertsandNotices/ucm262435.htm>
13. Feola A, Abramowitch S, Jallah Z, Stein S, Barone W, Palcsey S, Moalli P. Deterioration in biomechanical properties of the vagina following implantation of a high-stiffness prolapse mesh. *BJOG.* 2013; 120:224–32. [PubMed: 23240801]
14. Liang R, Abramowitch S, Knight K, Palcsey S, Nolfi A, Feola A, Moalli P. Vaginal degeneration following implantation of synthetic mesh with increased stiffness. *BJOG.* 2013; 120:233–43. [PubMed: 23240802]
15. Badylak SF, Freytes DO, Gilbert TW. Reprint of: Extracellular matrix as a biological scaffold material: Structure and function. *Acta Biomater.* 2015; 23(Suppl):S17–26. [PubMed: 26235342]
16. Badylak SF, Tullius R, Kokini K, Shelbourne KD, Klootwyk T, Voytik SL, Kraine MR, Simmons C. The use of xenogeneic small intestinal submucosa as a biomaterial for Achilles tendon repair in a dog model. *J Biomed Mater Res.* 1995; 29:977–85. [PubMed: 7593041]
17. DeJardin LM, Arnoczky SP, Ewers BJ, Haut RC, Clarke RB. Tissue-engineered rotator cuff tendon using porcine small intestine submucosa. Histologic and mechanical evaluation in dogs. *Am J Sports Med.* 2001; 29:175–84. [PubMed: 11292042]
18. Liang R, Woo SL, Takakura Y, Moon DK, Jia F, Abramowitch SD. Long-term effects of porcine small intestine submucosa on the healing of medial collateral ligament: a functional tissue engineering study. *J Orthop Res.* 2006; 24:811–9. [PubMed: 16514641]
19. Eilber KS, Alperin M, Khan A, Wu N, Pashos CL, Clemens JQ, Anger JT. Outcomes of vaginal prolapse surgery among female Medicare beneficiaries: the role of apical support. *Obstet Gynecol.* 2013; 122:981–7.
20. Lowder JL, Park AJ, Ellison R, Ghetti C, Moalli P, Zyczynski H, Weber AM. The role of apical vaginal support in the appearance of anterior and posterior vaginal prolapse. *Obstet Gynecol.* 2008; 111:152–7. [PubMed: 18165404]
21. Summers A, Winkel LA, Hussain HK, DeLancey JO. The relationship between anterior and apical compartment support. *Am J Obstet Gynecol.* 2006; 194:1438–43. [PubMed: 16579933]
22. Higgs PJ, Chua HL, Smith AR. Long term review of laparoscopic sacrocolpopexy. *BJOG.* 2005; 112:1134–8. [PubMed: 16045530]
23. Iglesia CB, Fenner DE, Brubaker L. The use of mesh in gynecologic surgery. *Int Urogynecol J Pelvic Floor Dysfunct.* 1997; 8:105–15. [PubMed: 9297599]

24. Benson JT, Lucente V, McClellan E. Vaginal versus abdominal reconstructive surgery for the treatment of pelvic support defects: a prospective randomized study with long-term outcome evaluation. *Am J Obstet Gynecol.* 1996; 175:1418–21. discussion 21–2. [PubMed: 8987919]
25. Afaneh C, Abelson J, Schattner M, Janjigian YY, Ilson D, Yoon SS, Strong VE. Esophageal reinforcement with an extracellular scaffold during total gastrectomy for gastric cancer. *Annals of Surgical Oncology.* 2015; 22:1252–7. [PubMed: 25319574]
26. Fleming ME, Bharmal H, Valerio I. Regenerative medicine applications in combat casualty care. *Regenerative Medicine.* 2014; 9:179–90. [PubMed: 24750059]
27. Remlinger NT, Gilbert TW, Yoshida M, Guest BN, Hashizume R, Weaver ML, Wagner WR, Brown BN, Tobita K, Wearden PD. Urinary bladder matrix promotes site appropriate tissue formation following right ventricle outflow tract repair. *Organogenesis.* 2013; 9:149–60. [PubMed: 23974174]
28. Rommer EA, Peric M, Wong A. Urinary bladder matrix for the treatment of recalcitrant nonhealing radiation wounds. *Advances in Skin & Wound Care.* 2013; 26:450–5. [PubMed: 24045565]
29. Freytes DO, Badylak SF, Webster TJ, Geddes LA, Rundell AE. Biaxial strength of multilaminated extracellular matrix scaffolds. *Biomaterials.* 2004; 25:2353–61. [PubMed: 14741600]
30. Feola A, Abramowitch S, Jones K, Stein S, Moalli P. Parity negatively impacts vaginal mechanical properties and collagen structure in rhesus macaques. *Am J Obstet Gynecol.* 2010; 203:595, e1–8.
31. Moalli PA, Shand SH, Zyczynski HM, Gordy SC, Meyn LA. Remodeling of vaginal connective tissue in patients with prolapse. *Obstet and Gynecol.* 2005; 106:953–63.
32. Rubod C, Boukerrou M, Brieu M, Dubois P, Cosson M. Biomechanical properties of vaginal tissue. Part 1: new experimental protocol. *J Uro.* 2007; 178:320–5. discussion 5.
33. Woo SL, Orlando CA, Camp JF, Akeson WH. Effects of postmortem storage by freezing on ligament tensile behavior. *J Biomechanics.* 1986; 19:399–404.
34. Gilbert TW, Stewart-Akers AM, Simmons-Byrd A, Badylak SF. Degradation and remodeling of small intestinal submucosa in canine Achilles tendon repair. *J Bone Joint Surg Am.* 2007; 89:621–30. [PubMed: 17332112]
35. Jallah Z, Liang R, Feola A, Barone W, Palcsey S, Abramowitch SD, Yoshimura N, Moalli P. The impact of prolapse mesh on vaginal smooth muscle structure and function. *BJOG.* 2016; 123:1076–85. [PubMed: 26301457]
36. Brown BN, Mani D, Nolfi AL, Liang R, Abramowitch SD, Moalli PA. Characterization of the host inflammatory response following implantation of prolapse mesh in rhesus macaque. *Am J Obstet Gynecol.* 2015; 213:668, e1–10. [PubMed: 26259906]
37. Nolfi AL, Brown BN, Liang R, Palcsey SL, Bonidie MJ, Abramowitch SD, Moalli PA. Host response to synthetic mesh in women with mesh complications. *Am J Obstet Gynecol.* 2016; 215:206, e1–8. [PubMed: 27094962]
38. Blumenkrantz N, Asboe-Hansen G. An automated procedure for quantitative determination of hydroxyproline. *Clin Biochem.* 1974; 7:251–7. [PubMed: 4426121]
39. Shiraishi K, Matsuzaki K, Matsumoto A, Hashimoto Y, Iba K. Development of a robust LC-MS/MS method for determination of desmosine and isodesmosine in human urine. *J Oleo Sci.* 2010; 59:431–9. [PubMed: 20625235]
40. Perla-Kajan J, Gryszczynska A, Mielcarek S, Jakubowski H. Cation exchange HPLC analysis of desmosines in elastin hydrolysates. *Anal Bioanal Chem.* 2011; 401:2473–9. [PubMed: 21887606]
41. Covault HP, Lubrano T, Dietz AA, Rubinstein HM. Liquid-chromatographic measurement of elastin. *Clin Chem.* 1982; 28:1465–8. [PubMed: 7083557]
42. Starcher BC, Galione MJ. Purification and comparison of elastins from different animal species. *Anal Biochem.* 1976; 74:441–7. [PubMed: 822746]
43. Muller G, Hanschke M. Quantitative and qualitative analyses of proteoglycans in cartilage extracts by precipitation with 1,9-dimethylmethylene blue. *Connect Tissue Res.* 1996; 33:243–8. [PubMed: 8834441]
44. Sykes B, Puddle B, Francis M, Smith R. The estimation of two collagens from human dermis by interrupted gel electrophoresis. *Biochemical and biophysical research communications.* 1976; 72:1472–80. [PubMed: 793589]

45. Brown BN, Valentin JE, Stewart-Akers AM, McCabe GP, Badylak SF. Macrophage phenotype and remodeling outcomes in response to biologic scaffolds with and without a cellular component. *Biomaterials*. 2009; 30:1482–91. [PubMed: 19121538]
46. Brown BN, Londono R, Tottey S, Zhang L, Kukla KA, Wolf MT, Daly KA, Reing JE, Badylak SF. Macrophage phenotype as a predictor of constructive remodeling following the implantation of biologically derived surgical mesh materials. *Acta biomater*. 2012; 8:978–87. [PubMed: 22166681]
47. Sicari BM, Agrawal V, Siu BF, Medberry CJ, Dearth CL, Turner NJ, Badylak SF. A murine model of volumetric muscle loss and a regenerative medicine approach for tissue replacement. *Tissue Eng Part A*. 2012; 18:1941–8. [PubMed: 22906411]
48. Agrawal V, Tottey S, Johnson SA, Freund JM, Siu BF, Badylak SF. Recruitment of progenitor cells by an extracellular matrix cryptic peptide in a mouse model of digit amputation. *Tissue Eng Part A*. 2011; 17:2435–43. [PubMed: 21563860]
49. Zantop T, Gilbert TW, Yoder MC, Badylak SF. Extracellular matrix scaffolds are repopulated by bone marrow-derived cells in a mouse model of achilles tendon reconstruction. *J Orthop Res*. 2006; 24:1299–309. [PubMed: 16649228]
50. Nieponice A, Gilbert TW, Johnson SA, Turner NJ, Badylak SF. Bone marrow-derived cells participate in the long-term remodeling in a mouse model of esophageal reconstruction. *J Surg Res*. 2013; 182:e1–7. [PubMed: 23069684]
51. Davis GE, Bayless KJ, Davis MJ, Meininger GA. Regulation of tissue injury responses by the exposure of matricryptic sites within extracellular matrix molecules. *Am J Pathol*. 2000; 156:1489–98. [PubMed: 10793060]
52. Badylak S, Kokini K, Tullius B, Whitson B. Strength over time of a resorbable bioscaffold for body wall repair in a dog model. *J Surg Res*. 2001; 99:282–7. [PubMed: 11469898]
53. Otto LN, Slayden OD, Clark AL, Brenner RM. The rhesus macaque as an animal model for pelvic organ prolapse. *Am J Obstet Gynecol*. 2002; 186:416–21. [PubMed: 11904600]

Statement of Significance

Pelvic organ prolapse is a common condition related to failure of the supportive soft tissues of the vagina; particularly at the apex and mid-vagina. Few studies have investigated methods to regenerate these failed structures. The overall goal of the study was to determine the feasibility of utilizing a regenerative bioscaffold in prolapse applications to restore apical (level I) and lateral (level II) support to the vagina without negatively impacting vaginal structure and function. The significance of our findings is two fold: 1. Implantation of properly constructed extracellular matrix grafts promoted rebuilding of level I and level II support to the vagina and did not negatively impact the overall functional, morphological and biochemical properties of the vagina. 2. The presence of vaginal incisions in the transvaginal insertion of bioscaffolds may compromise vaginal structural integrity in the short term.

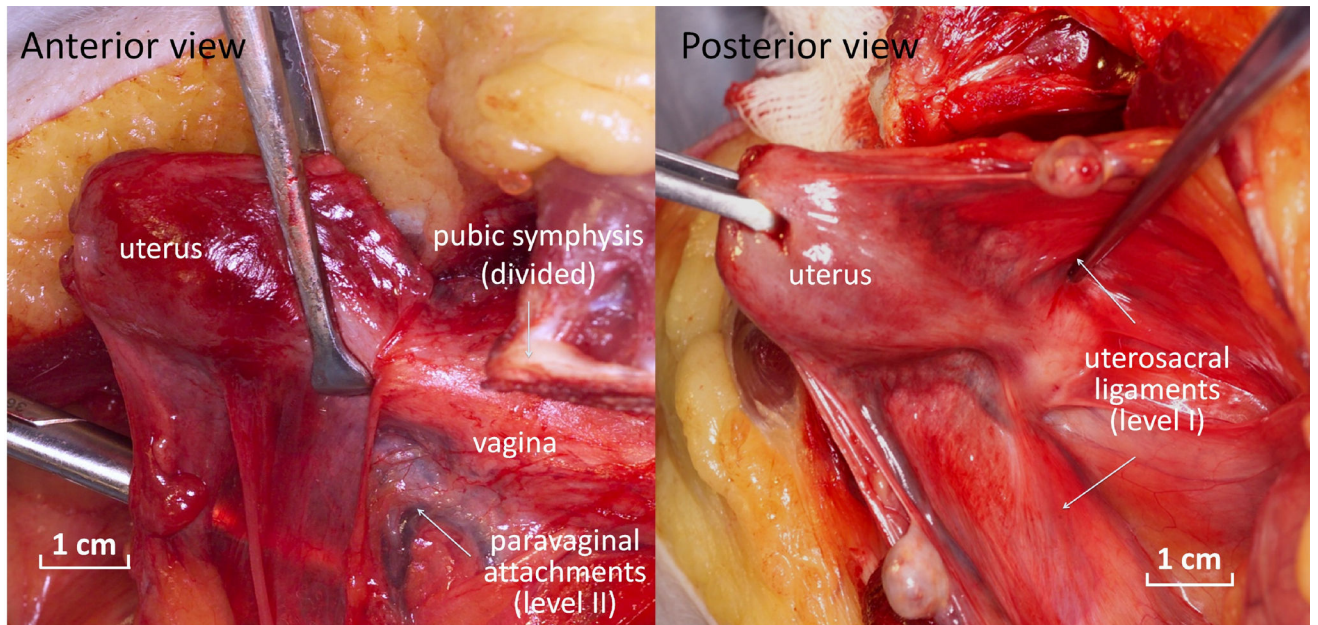


Figure 1. Normal pelvic organ support. In the normally supported vagina, lateral support is provided by the paravaginal attachments to the pelvic sidewall (level II support) which are best visualized with disruption of the pubic symphysis as shown in anterior view. The top of the vagina is pulled up and back toward the sacrum by the uterosacral ligaments (level I support) as depicted in the posterior view of the uterus and vagina.

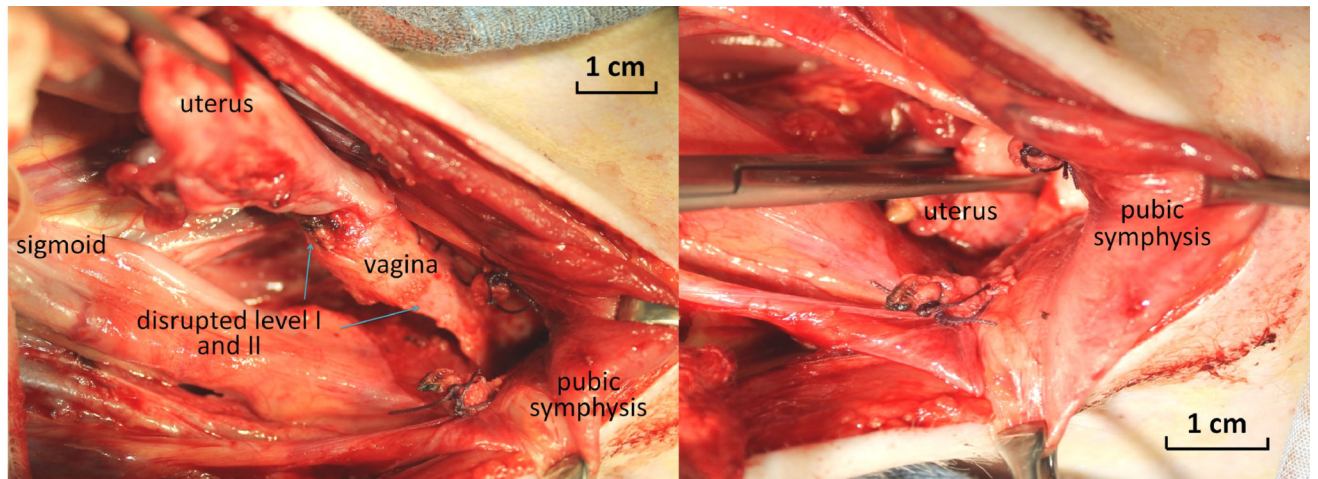


Figure 2. Surgical disruption of level I (uterosacral ligaments) and level II (paravaginal attachments). Prior to placement of the ECM bioscaffolds, level I and II support were disrupted surgically. A: demonstrating a complete absence of level I and level II support. B: demonstrating free movement of the uterus and vagina below the pubic symphysis and through the vaginal introitus mimicking pelvic organ prolapse.

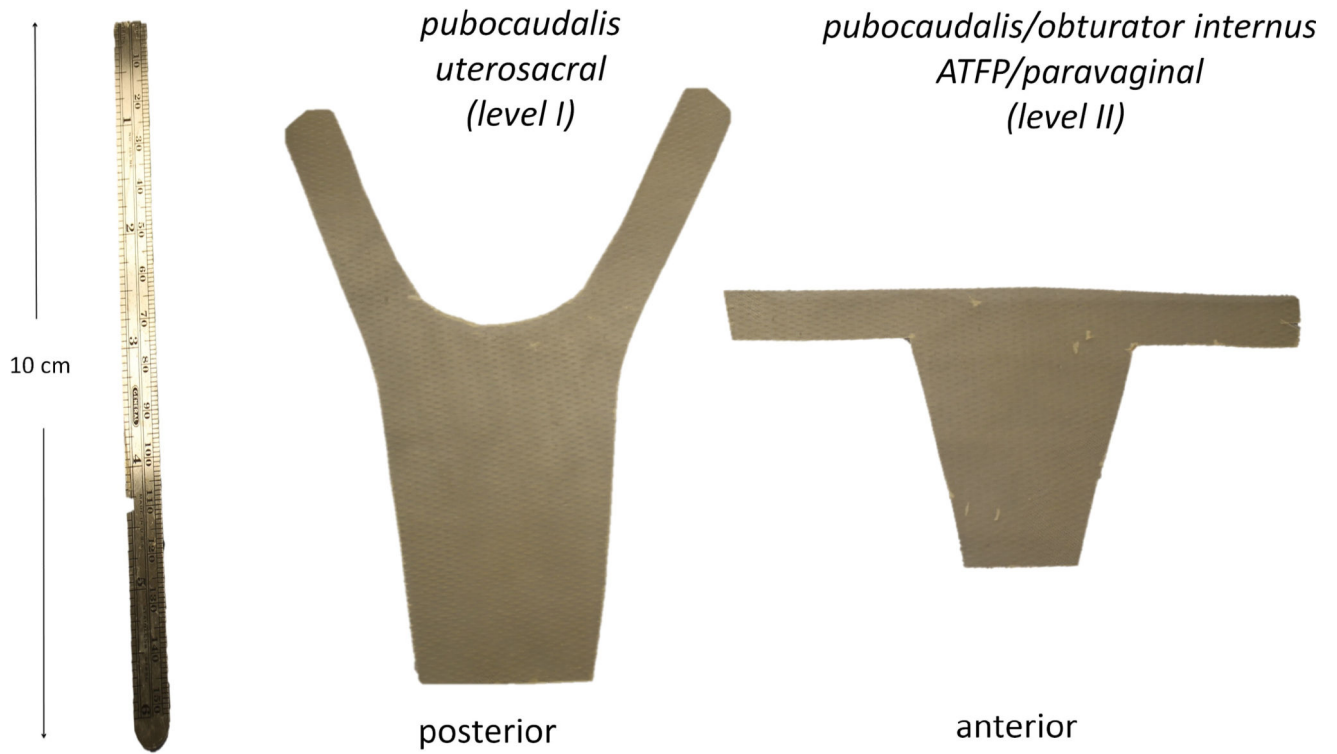


Figure 3.

Anterior and posterior templates made from the ECM bioscaffold. The body of the posterior scaffold covers the posterior vagina with arms that insert into the tendon of the pubocaudalis muscle immediately adjacent to the sacrum for regeneration of level I (apical) support. The anterior scaffold has a vaginal portion and arms to insert into the arcus tendineus fasciae pelvis at the junction of the pubocaudalis and obturator internus muscles for regeneration of level II (paravaginal) support.

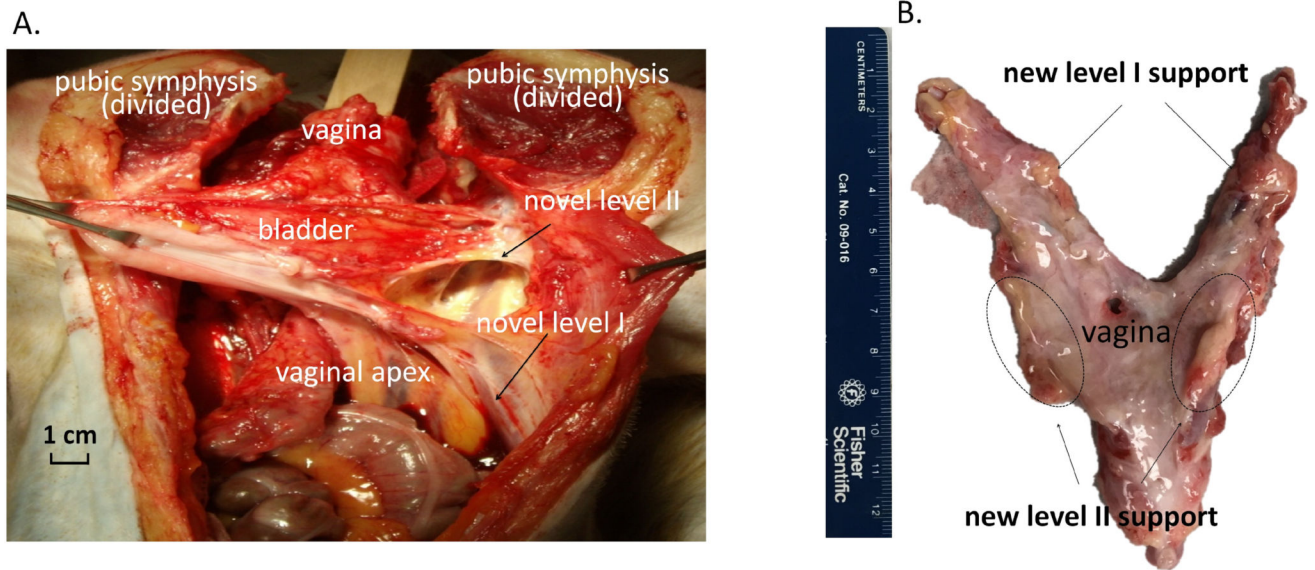


Figure 4. Gross morphology demonstrating newly formed tissues supporting the vaginal apex in the area of the uterosacral ligaments (level I) and newly formed tissues in the area of paravaginal attachments to the pelvic sidewall supporting the mid vagina (level II) at 3 months following the implantation of the EMC bioscaffolds. (A). In-vivo anatomy. (B). Morphology after dissection.

H & E staining

Immunofluorescence

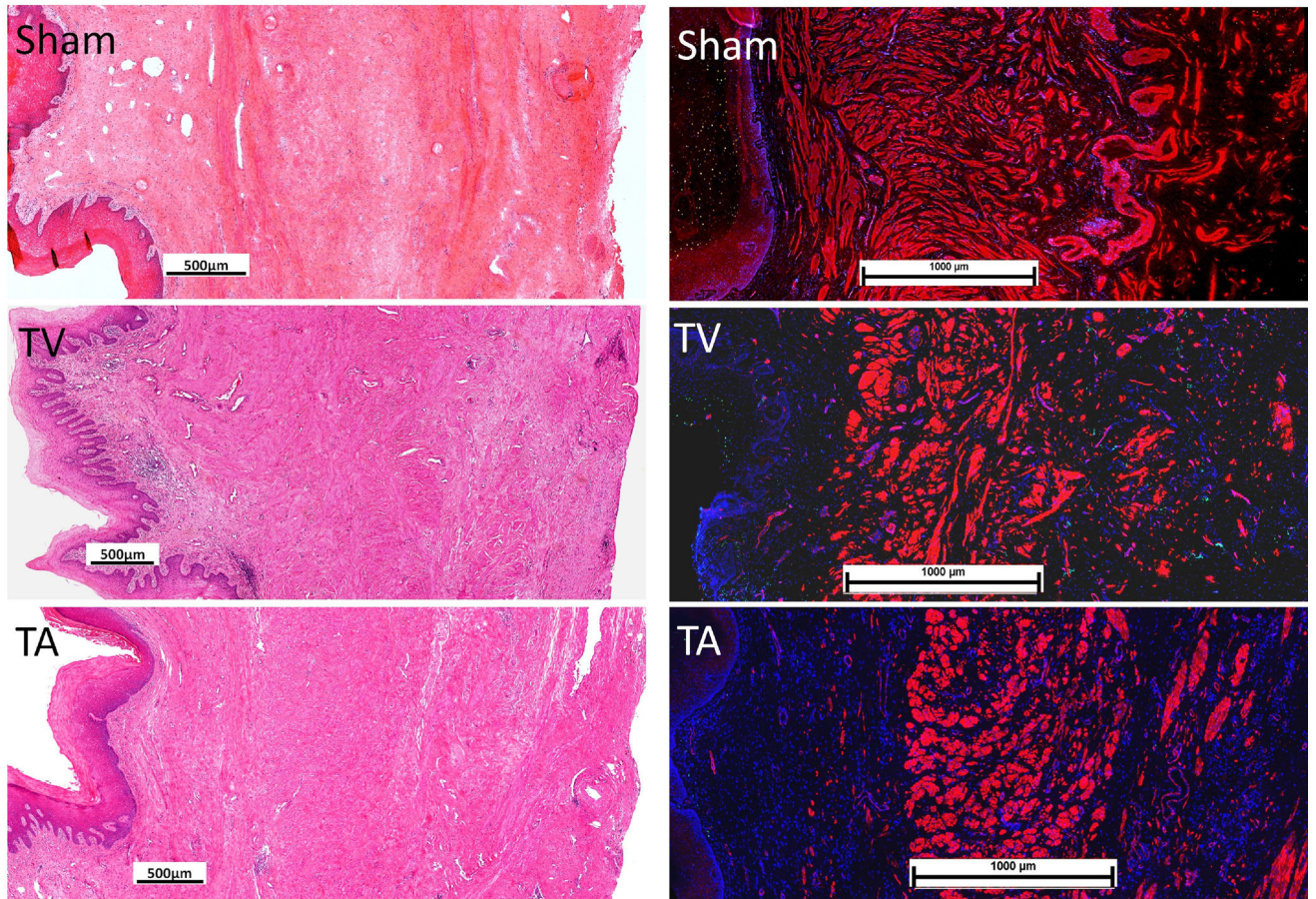


Figure 5. H&E staining (left panel) and immunofluorescent labeling (right panel) of α -smooth muscle actin (red), apoptosis (green) and nuclei (blue) at 3 months following the implantation of ECM bioscaffolds. TV: MatriStem transvaginal insertion; TA: MatriStem transabdominal insertion. Scale bars in H & E staining represent 500µm and scale bars in immunofluorescence represent 1000 µm.

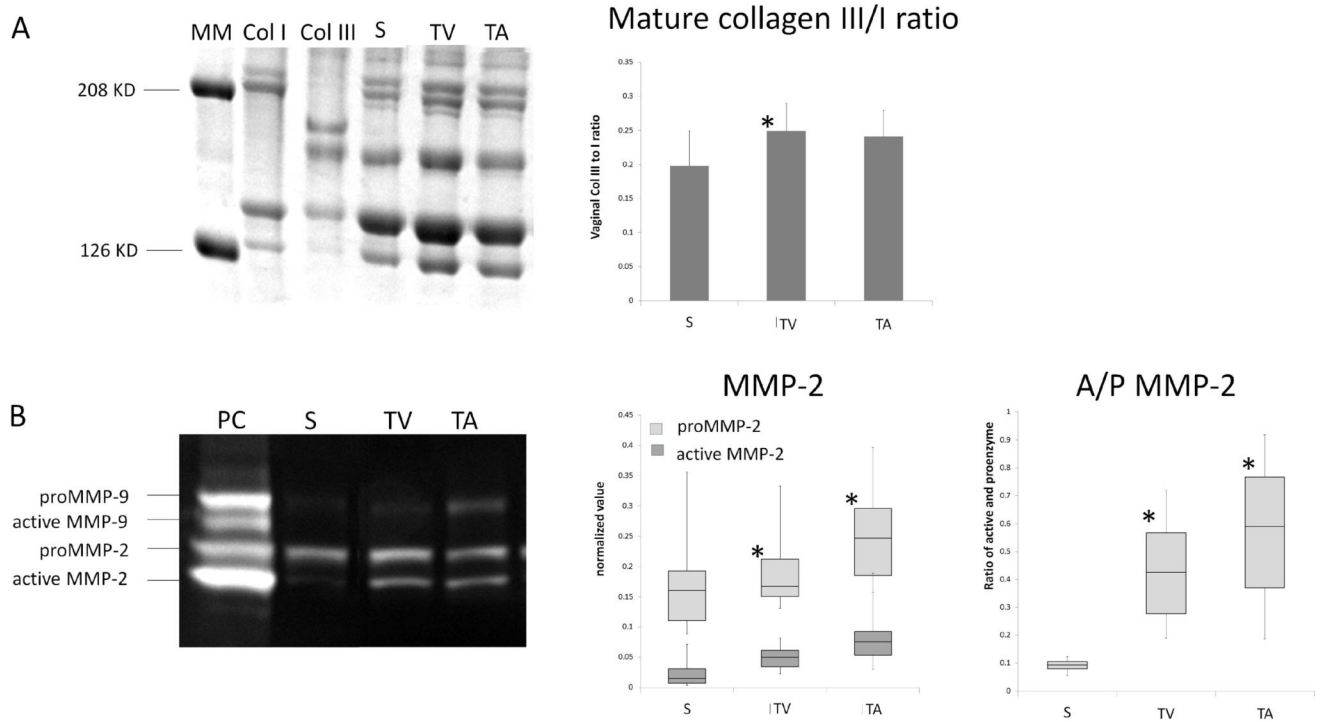


Figure 6.

A. SDS-PAGE results of mature collagen III/I ratio in vagina at 3 months following the implantation of ECM bioscaffolds. B. Zymography results of MMP –2 and –9 in vagina at 3 months following the implantation of ECM bioscaffolds. MM: Molecular marker; Col I: collagen I standard; Col III: collagen III standard; S: Sham; TV: MatriStem transvaginal insertion; TA: MatriStem transabdominal insertion; PC: positive control. * indicates statistical difference from Sham with $P < 0.05$.

Table 1

Demographics of non-human primates in the study. The values for age, gravidity and parity are expressed as median (1st quartile, 3rd quartile); the value for weight is expressed as mean \pm standard deviation. MatriStem TA: MatriStem implantation modeling transabdominal insertion (n=8) or MatriStem TV: MatriStem implantation modeling transvaginal insertion (n=8).

	Age	Weight (kg)	Gravidity	Parity
Sham	14.5 (10, 15.25)	7.5 \pm 1.6	2.5 (2, 6)	3.5 (2, 6)
MatriStem TA	8 (8, 8.25)	7.2 \pm 1.6	2 (1.75, 2.25)	2 (1.75, 2.25)
MatriStem TV	8 (8, 9)	7.0 \pm 1.6	2 (1.75, 3.25)	2 (1.75, 2.25)
p*	0.001	0.200	0.069	0.088

* indicates the comparison of overall p value among the groups

Biomechanical analysis of the vaginal wall after MatriStem implantation modeling transabdominal insertion (MatriStem TA, n=8) or transvaginal insertion (MatriStem TV, n=8) as compared to historical data for Sham [13]. Results are expressed as median (1st quartile, 3rd quartile). Post hoc P values represent comparisons between groups.

Table 2

	Stiffness (N/mm)	Ultimate Load (N)	Extension (mm)	Energy Absorbed (N/mm)	Thickness (mm)
Sham	35.8 (30.6, 49.5)	154.9 (95.8, 172.2)	11.7 (10.0, 12.8)	413.5 (248.1, 495.7)	4.7 (2.5, 9.2)
MatriStem TA	32.5 (30.2, 61.6)	163.1 (106.4, 222.9)	20.6 ^a (20.6, 24.0)	544.6 (289.1, 625.0)	5.8 (4.9, 6.6)
MatriStem TV	19.7 ^a (10.9, 24.6)	61.7 (36.1, 116.5)	19.4 (18.2, 23.2)	201.7 (141.5, 311.9)	4.5 (2.5, 6.6)
P [*]	0.061	0.127	0.035	0.12	0.50
Post hoc P					
TA vs. Sham	0.768	0.513	0.001	0.206	0.768
TV vs. Sham	0.042	0.093	0.958	0.263	0.313

* indicates the overall comparison among the groups

^a indicates $p < 0.05$ compared with Sham

Table 3

Functional and morphometric analysis of the vagina after MatriStem implantation modeling transabdominal insertion (MatriStem TA, n=8) or transvaginal insertion (MatriStem TV, n=8) as compared to historical data for Sham [13, 14]. Results are expressed as mean \pm standard deviation for subepithelium and muscularis thickness, or median (1st quartile, 3rd quartile) for contractile function and cell apoptosis quantification. Post hoc P values represent comparisons between groups. EFS: electrical field stimulation.

	Function		Morphometrics			Cell apoptosis (%)	
	contractility (mN/mm ²)	EFS (g/g)	subepithelium thickness (μ m)	Muscularis thickness (μ m)	subepithelium	muscularis	adventitia
Sham	0.23 (0.17, 0.35)	0.46 (0.27, 0.70)	522 \pm 189	1557 \pm 499	0.18 (0.12, 0.28)	0.02 (0.01, 0.03)	0.65 (0.47, 0.72)
MatriStem TA	0.19 (0.16, 0.22)	0.38 (0.23, 0.57)	509 \pm 140	1406 \pm 324	0.08 (0.08, 0.21)	0.07 (0.04, 0.20)	1.48 (0.42, 3.06)
MatriStem TV	0.14 (0.09, 0.34)	0.58 (0.26, 0.85)	855 \pm 389	1518 \pm 218	0.19 (0.02, 0.65)	0.08 (0.03, 0.09)	0.93 (0.70, 1.24)
P*	0.154	0.797	0.064	0.747	0.940	0.792	0.280
Post hoc P							
TA vs. Sham	0.505	0.721	0.993	0.685	0.852	0.491	0.366
TV vs. Sham	0.189	0.613	0.051	0.978	0.950	0.950	0.166

* indicates the overall comparison among the groups

Table 4

Biochemical analysis of the vagina after MatriStem implantation modeling transabdominal insertion (MatriStem TA, n=8) or transvaginal insertion (MatriStem TV, n=8) as compared to historical data for Sham [14]. Results are expressed as mean \pm standard deviation. Post hoc P values represent comparisons between groups.

	Biochemistry analysis			
	Collagen (% of dry weight)	Elastin (% of dry weight)	GAG (% of dry weight)	Col III/I ratio
Sham	48.3 \pm 8.6	16.5 \pm 4.4	1.35 \pm 0.33	0.20 \pm 0.05
MatriStem TA	43.6 \pm 4.6	18.5 \pm 4.8	1.64 \pm 0.30	0.24 \pm 0.04
MatriStem TV	37.7 \pm 7.8 ^a	16.4 \pm 3.3	1.45 \pm 0.18	0.25 \pm 0.04 ^a
p*	0.016	0.534	0.107	0.036
Post hoc P				
TA vs. Sham	0.304	0.527	0.068	0.088
TV vs. Sham	0.008	0.989	0.675	0.038

* indicates the overall comparison among the groups

^a indicates $p < 0.05$ compared with Sham